PHYSICAL REVIEW D **83,** 074015 (2011)

Fourth generation bound states

Koji Ishiwata and Mark B. Wise
California Institute of Technology, Pasadena, California, 91125 USA
(Received 9 March 2011; published 14 April 2011)

We investigate the spectrum and wave functions of $\bar{q}'q'$ bound states for heavy fourth generation quarks (q') that have a very small mixing with the three observed generations of standard model quarks. Such bound states come with different color, spin and flavor quantum numbers. Since the fourth generation Yukawa coupling, $\lambda_{q'}$, is large we include all perturbative corrections to the potential between the heavy quark and antiquark of order $\lambda_{q'}^2 N_c/16\pi^2$ where N_c is the number of colors, as well as relativistic corrections suppressed by $(v/c)^2$. We find that the lightest fourth generation quark masses for which a bound state exists for color octet states. For the color singlet states, which always have a bound state, we analyze the influence that the Higgs couplings have on the size and binding energy of the bound states.

DOI: 10.1103/PhysRevD.83.074015 PACS numbers: 14.65.Jk, 12.60.−i

I. INTRODUCTION

Among the mysteries of nature is the number of generations. We observe three generations, however there could be a fourth generation if the masses of the quarks and leptons are beyond our present experimental reach. Data from the Tevatron (under some circumstances) restricts the masses of the t' and b' quarks in a fourth generation to be greater than about 350 GeV. For some recent studies see [1]. A strong constraint on the masses of fourth generation quarks comes from precision electroweak physics. Heavy fourth generation quarks contribute to the S parameter and to the ρ parameter. Their large contribution to the S parameter rules out a fourth generation with degenerate t' and b' quarks. However they also contribute to the ρ parameter and Kribs *et. al.* showed that an acceptable combined fit to precision electroweak data can be achieved, for example, with a mass splitting of about 50 GeV between fourth generation quarks in the mass range 350–700 GeV [2]. See also the earlier work in [3]. Large splitting may also be possible [4]. For a more recent discussion of electroweak fits see [5–7].

In addition, there is a ''unitarity upper limit'' on fourth generation quark mass of about 500 GeV [8,9]. This does not, however, necessarily forbid heavier quark masses. Rather it indicates that higher order perturbative corrections become important at this mass [10]. Dynamical considerations rather than unitarity give an upper bound of about 3 TeV. This is similar to the upper bound on the Higgs scalar mass [11,12].

A heavy fourth generation can destabilize electroweak symmetry breaking (see [13] for a review). According to the recent work in [14], if there is no new physics (apart from the fourth generation) below a TeV, the Higgs mass should be roughly equal to or larger than a fourth generation quark mass in order to avoid the instability. Of course there could be new particles beyond the fourth generation fermions below a TeV that get a large part of their masses from electroweak symmetry breaking. For example, scalars S that have a term in the scalar potential $gS^\dagger SH^\dagger H$ get a contribution to the squares of their masses equal to $gv^2/2$ ($v \simeq 246$ GeV) and such interactions could help stabilize the Higgs potential.

It is easy to imagine simple physical mechanisms that suppress the mass mixing between the heavy fourth generation quarks and the three generations of standard model quarks. For example, the fourth generation quarks and leptons could have a different value for $B - L$ than the standard three generations. (Here B and L are the baryon number and lepton number.) If the $B - L$ violation is small then the mixing between fourth generation quarks and the standard three generations is suppressed. For example, fourth generation quarks and leptons with both a baryon and lepton number minus 3 times those of the ordinary three generations of quarks and leptons can cancel the baryon and lepton number anomalies, allowing those symmetries to be gauged [15].

Heavy fourth generation quarks feel a strong attractive force from the Higgs exchange in both the $\bar{q}'q'$ and $q'q'$ channels that gives rise to bound states [16]. If the fourth generation quarks have a very small mixing with the ordinary quarks, they can be long enough lived that bound $\bar{q}'q'$ states decay through $\bar{q}'q'$ annihilation and not via q' decay to a lower generation quark and a W boson. In this case the production of these bound states at the LHC may have important experimental consequences. Furthermore the $q'q'$ bound states may be long very lived. References [16–19] discuss some other interesting possible physical consequences of a heavy fourth generation.

In this paper we focus on the physics of the $\bar{q}'q'$ states. Here we explore the role of perturbative corrections suppressed by $N_c\lambda_{q'}^2/16\pi^2$, and α_s (here N_c is the number of color and α_s is strong coupling constant), as well as relativistic corrections on the spectrum and wave functions of the $\bar{q}'q'$ bound states. We find that the perturbative and relativistic corrections have a significant impact on wave functions and spectrum of $\bar{q}'q'$ bound states.

The $\bar{q}'q'$ bound states can be in a color singlet or color octet configuration. For the color octet states we find the lightest fourth generation quark masses for which a bound state exists. In any color singlet configuration there is always a bound state. Therefore we discuss the impact of the Higgs couplings to the heavy quarks on the shape of the wave functions for the bound states and the bound state binding energies. In the numerical analysis, we sometimes show results for values of $m_{q'}$ that are below the experimental limit of 350 GeV or above 500 GeV where we expect perturbation theory to be of limited use. Our excursion into these regimes is for pedagogical reasons and does not mean we dismiss the constraints from experiment or the limitations imposed by perturbativity.

II. HAMILTONIAN

Since precision electroweak physics favors a small value for $|(m_{b'} - m_{t'})/(m_{b'} + m_{t'})|$ (here $m_{t'}$ and $m_{b'}$ are masses of t' and b', respectively), we work in the limit where the heavy fourth generation quark masses are equal, i.e., $m_{t'} = m_{b'} = m_{q'}$. It is straightforward to add in the effects of the difference between the heavy fourth generation quark masses. (We discuss the impact of a fourth generation quark mass splitting at the end of this paper.) Then the leading order Hamiltonian for heavy quark bound states from a Higgs scalar exchange is

$$H^{(0)} = \frac{\mathbf{p}^2}{m_{q'}} - (\sqrt{2}G_F m_{q'}^2)\frac{e^{-m_h r}}{4\pi r}, \tag{1}$$

where $\mathbf{p}$ and $\mathbf{x}(r = |\mathbf{x}|)$ are momentum and relative coordinates in the center of mass frame, and m_h is the Higgs scalar mass. In momentum space the leading potential from tree-level Higgs exchange is

$$\tilde{V}(\mathbf{p}) = -\frac{\sqrt{2}G_F m_{q'}^2}{\mathbf{p}^2 + m_h^2}. \tag{2}$$

Here we have expressed the heavy quark Yukawa coupling, $\lambda_{q'}$, in terms of the Fermi constant G_F and the heavy fourth generation quark mass. Using the variational method based on a trial wave function $\Psi \propto e^{-r/a}$ [16] and taking, for example, $m_h = 130$ GeV, this Hamiltonian has an S-wave bound state for $m_{q'} > 583$ GeV. In this section, we compute perturbative corrections and relativistic corrections to the Hamiltonian. We also give the QCD potential at order of α_s for color singlet and color octet configurations.

A. Perturbative corrections to the potential enhanced by the number of colors

Here we include perturbative corrections to the potential of $\bar{q}'q'$ state of order $N_c\lambda_{q'}^2/16\pi^2$. These arise from the heavy fourth generation quark contribution to the Higgs boson self-energy $\Sigma^h(p^2)$. They will give a correction to the leading order potential. For pedagogical reasons we also include terms proportional to the top quark Yukawa squared but set the other quark masses to zero. (In this section, we express formulas assuming $m_h \le 2m_t$. However, the top quark contribution is negligible in the numerical results.) Expressing the Yukawa coupling squared in terms of the quark mass squared and G_F, all the perturbative corrections enhanced by a factor of N_c come from the Higgs scalar self-energy and the W-boson vacuum polarization.

Let us consider the Higgs propagator. It is determined by the one-loop calculation of a quark loop diagram (see left on Fig. 1),

$$D_h(p^2) = \frac{i(1 + \delta^h)}{p^2 - m_h^2 - \bar{\Sigma}^h(p^2)}, \tag{3}$$

with

$$\bar{\Sigma}^h(p^2) = \sum_{q=t',b',t} \frac{\lambda_q^2 N_c}{16\pi^2}\Big[L^q(p^2) - L^q_<(m_h^2) - (p^2 - m_h^2)\frac{dL^q_<(p^2)}{dp^2}\Big|_{p^2=m_h^2}\Big]. \tag{4}$$

Here the functions L^q and $L^q_<$ are defined by

$$L^q(p^2) = \begin{cases} L^q_>(p^2) = p^2\beta^3\Big[\log\Big(\frac{1+\beta}{1-\beta}\Big) - i\pi\Big] & 4m_q^2 < p^2 \\ L^q_<(p^2) = -2p^2 b^3 \tan^{-1}\Big(\frac{1}{b}\Big) & 0 < p^2 < 4m_q^2, \\ L^q_-(p^2) = p^2\beta^3\log\Big(\frac{\beta+1}{\beta-1}\Big) & p^2 < 0 \end{cases} \tag{5}$$

where

$$\beta = \sqrt{1 - \frac{4m_q^2}{p^2}}, \quad b = \sqrt{\frac{4m_q^2}{p^2} - 1} \text{ and } x_q = \frac{m_q^2}{m_h^2}. \tag{6}$$

The derivative of $L^q_<(p^2)$ evaluated at $p^2 = m_h^2$ is

$$\frac{dL^q_<(p^2)}{dp^2}\Big|_{p^2=m_h^2} = 1 - 4x_q + 2\sqrt{4x_q - 1}(1 + 2x_q) \times \tan^{-1}(1/\sqrt{4x_q - 1}). \tag{7}$$

Finally, using $\overline{\text{MS}}$ subtraction (with the number of space-time dimensions $n = 4 - \epsilon$), δ^h is given as

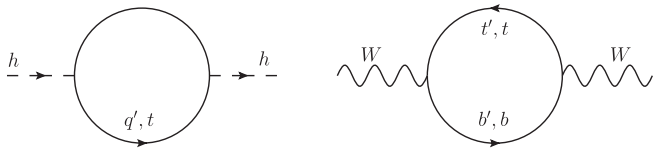

FIG. 1. Diagrams of Higgs self-energy (left) and W boson vacuum polarization (right).

$$\delta^h = \frac{d\Sigma^h(p^2)}{dp^2}\bigg|_{p^2=m_h^2} = \sum_{q=t',b',t} \frac{\lambda_q^2 N_c}{16\pi^2}\bigg[-\bigg(\frac{2}{\epsilon}+\log\bigg(\frac{\mu^2}{m_q^2}\bigg)\bigg)-2+\frac{dL_<^q(p^2)}{dp^2}\bigg|_{p^2=m_h^2}\bigg]. \tag{8}$$

Expanding the factor $\overline{\Sigma}^h(p^2)$ in a power series in, $p^2 - m_h^2$, it is clear from its definition in Eq. (4) that it first contributes at order $(p^2 - m_h^2)^2$.

In the numerator of the Higgs propagator the factor δ^h is divergent. This divergence is cancelled in the potential if we express the fourth generation quark Yukawa couplings $\lambda_{q'}^2$ in terms of $G_F m_{q'}^2$. The resulting correction to the Fourier transform of the potential is

$$\tilde{V}_{\text{pert}}(\mathbf{p}) = -\frac{\sqrt{2}G_F m_{q'}^2 \delta}{\mathbf{p}^2 + m_h^2}. \tag{9}$$

Here the perturbative corrections in the denominator of the Higgs propagator can be negligible. This arises because of a cancellation between the three terms in Eq. (4). Here we have used the expansions

$$L_<^q(m_h^2) = m_q^2\bigg(-8 + \frac{8}{3}\frac{m_h^2}{m_q^2} + \ldots\bigg), \tag{10}$$

$$\frac{dL_<^q(p^2)}{dp^2}\bigg|_{p^2=m_h^2} = -\frac{8}{3} + \ldots, \tag{11}$$

$$L_-^q(-\mathbf{p}^2) = m_q^2\bigg(-8 - \frac{8}{3}\frac{\mathbf{p}^2}{m_q^2} + \ldots\bigg). \tag{12}$$

Even though the expansions we used in Eqs. (10)–(12) are applicable for $m_h \ll 2m_{q'}$, we have checked numerically that the denominator of Eq. (9) is a good approximation when $m_h \sim m_{q'}$. On the other hand, the factor δ in the numerator of the potential is given by

$$\delta = \delta^h + \frac{\Pi_{WW}^T(0)}{M_W^2}. \tag{13}$$

Here $\Pi_{WW}^T(p^2)$ is the transverse part of W boson vacuum polarization $\Pi_{WW,\mu\nu}(p^2)$, defined by $\Pi_{WW,\mu\nu}(p^2) = g_{\mu\nu}\Pi_{WW}^T(p^2) + \cdots$. For $\Pi_{WW}^T(0)$ there are two contributions (see right on Fig. 1), $\Pi_{WW}^T(0) = \Pi_{WWq'}^T(0) + \Pi_{WWt}^T(0)$ and these are

$$\Pi_{WWq'}^T(0)/M_W^2 = \frac{2\lambda_{q'}^2 N_c}{16\pi^2}\bigg(\frac{2}{\epsilon} + \ln\bigg(\frac{\mu^2}{m_{q'}^2}\bigg)\bigg), \tag{14}$$

$$\Pi_{WWt}^T(0)/M_W^2 = \frac{\lambda_t^2 N_c}{16\pi^2}\bigg(\frac{2}{\epsilon} + \ln\bigg(\frac{\mu^2}{m_t^2}\bigg) + \frac{1}{2}\bigg). \tag{15}$$

Using the above results, one obtains

$$\delta = \frac{2N_c}{48\pi^2}\sum_{q=t',b',t}\lambda_q^2 + \frac{N_c}{32\pi^2}\lambda_t^2 = \frac{\sqrt{2}G_F}{2\pi^2}m_{q'}^2 + \frac{7\sqrt{2}G_F}{16\pi^2}m_t^2. \tag{16}$$

Here we take $N_c = 3$. The divergences in δ^h and $\Pi_{WW}^T(0)$ canceled. Equations (9) and (16) are the main results of this section.

B. Relativistic corrections

Relativistic corrections to the potential come from expanding the spinors in the Higgs scalar exchange diagram and from including the contributions from longitudinal gauge bosons and the "fictitious scalars" in R_ξ gauge. We choose $\xi = 1$ so that the longitudinal gauge boson contribution vanishes. The corrections appropriate for the ground S-wave bound states are given here. For discussions of how the relativistic corrections to the potential are derived from Feynman diagrams see Refs. [20,21].

Expanding the spinors for the t-channel Higgs exchange diagram (shown in Fig. 2) gives the relativistic correction to the potential,

$$\tilde{V}_{\text{rel.Higgs}}(\mathbf{p}) = -\frac{\sqrt{2}G_F}{4}\bigg(\frac{\mathbf{p}^2}{\mathbf{p}^2 + m_h^2}\bigg). \tag{17}$$

Neutral fourth generation bound states can exist in the flavor states $\bar{t}'t'$ and $\bar{b}'b'$, can be in color singles (**1**) and octets (**8**), and furthermore they can have zero and one spins. Since we are working in the limit $m_{t'} = m_{b'}$, it is convenient to decompose the flavor structure into heavy quark isospin $I = 0$ (i.e., $(\bar{t}'t' + \bar{b}'b')/\sqrt{2}$) and $I = 1$ (i.e., $(\bar{t}'t' - \bar{b}'b')/\sqrt{2}$). So far the contributions to the Hamiltonian have not depended on the bound states heavy quark isospin, color and spin quantum numbers. However, the contributions we consider now do depend on these quantum numbers. We therefore attach the superscript, $C =$ color, $I =$ heavy quark isospin, $S =$ heavy quark spin) to the potential. Since these eight states characterized by (C, I, S) do not necessarily form bound states, hereafter we call them "channels".

Exchange of the neutral " fictitious scalar" (which we call P^0) in the t channel (left on Fig. 3) gives spin-dependent potential, but is independent of the color and flavor. We find that

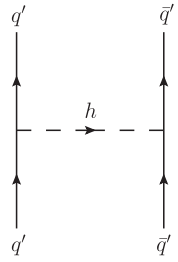

FIG. 2. t-channel Higgs exchange.

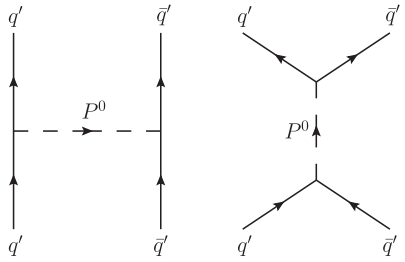

FIG. 3. s- and t-channel neutral fictitious scalar exchange.

$$\tilde{V}^{(S)}_{P^0,t\text{-channel}}(\mathbf{p}) = \frac{\sqrt{2}G_F}{4}\frac{\mathbf{p}^2}{\mathbf{p}^2 + M_Z^2}\Omega(S), \tag{18}$$

where M_Z is Z boson mass, and for spin one, $\Omega(1) = -1/3$, and for spin zero, $\Omega(0) = 1$. This contribution is attractive in the spin one channel and repulsive in the spin zero channel. The s-channel P^0 exchange (left on Fig. 3), on the other hand, gives a repulsive potential which only occurs in the $(\mathbf{1}, 1, 0)$ channel,

$$\tilde{V}^{(\mathbf{1},1,0)}_{P^0,s\text{-channel}}(\mathbf{p}) = \frac{3\sqrt{2}G_F}{1 - M_Z^2/(4m_{q'}^2)}. \tag{19}$$

It is enhanced by a factor of $N_c = 3$, compared with other relativistic corrections to the potential.

The final relativistic correction to the potential comes from the t-channel exchange of the charged fictitious scalar P^+, which is depicted in Fig. 4. It is independent of color but depends on spin and on flavor since it mixes the $\bar{t}'t'$ and $\bar{b}'b'$ channel. We find that

$$\tilde{V}^{(S)}_{P^+}(\mathbf{p}) = \pm\frac{\sqrt{2}G_F}{2}\frac{\mathbf{p}^2}{\mathbf{p}^2 + M_W^2}\Omega(S), \tag{20}$$

where M_W is the W-boson mass. Here plus and minus signs correspond to $I = 1$ and 0 channels, respectively.

Finally there is the usual relativistic correction to the kinetic energy:

$$T_{\text{rel}} = -\frac{\mathbf{p}^2}{m_{q'}}\left(\frac{\mathbf{p}^2}{4m_{q'}^2}\right). \tag{21}$$

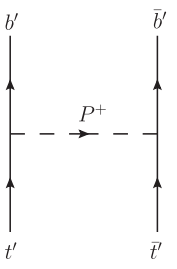

FIG. 4. t-channel charged fictitious scalar exchange.

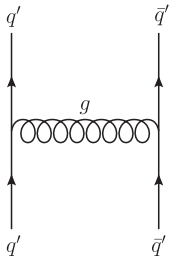

FIG. 5. Gluon exchange.

C. QCD Potential

There are also contributions to the potential from one-gluon exchange (Fig. 5). They are attractive in the color singlet channel and repulsive in the color octet channel but are spin and flavor independent, and are given as

$$V^{(\mathbf{1})}_{\text{QCD}}(r) = -\frac{4}{3}\alpha_s\left(\frac{1}{r}\right), \tag{22}$$

$$V^{(\mathbf{8})}_{\text{QCD}}(r) = \frac{1}{6}\alpha_s\left(\frac{1}{r}\right). \tag{23}$$

There are always bound states in the color singlet channel because the strong interactions confine. In the octet channel there are no bound states without the Yukawa potential from the Higgs exchange. In our numerical work we evaluate α_s at the Z boson mass, $\alpha_s(M_Z) = 0.118$.

III. NUMERICAL RESULTS

In this section we discuss the ground state S-wave states in the various color, heavy flavor isospin, and spin channels. The Hamiltonian for this system is

$$H = H^{(0)} + H^{(1)}, \tag{24}$$

where

$$H^{(1)} = T_{\text{rel}} + V_{\text{pert}} + V_{\text{rel Higgs}} + V_{P^0,t\text{-channel}} + V_{P^0,s\text{-channel}} + V_{P^+} + V_{\text{QCD}}. \tag{25}$$

We use the variational method, minimizing $E[a] = \langle\psi|H|\psi\rangle/\langle\psi|\psi\rangle$ for trial wave functions $\psi \propto e^{-r/a}$. In order for the v/c expansion to make sense, we restrict our analysis to wave functions that give an expectation value for $\mathbf{p}^2/m_{q'}^2$ that is smaller than $1/3$. This ensures that higher order terms in the v/c expansion, which we have neglected, are not important. This means that

$$a^2 \geq 3/m_{q'}^2. \tag{26}$$

Before discussing the numerical results, we give the formula for $E[a]$ in each channel. The expectation values of the kinetic energy and the potential from the Higgs exchange and t-channel neutral fictitious scalar exchange give a common contribution for color singlet/octet and isospin zero/one channels. These are given by

$$E^{(S)}_{\rm com}[a] = \frac{1}{a}\Big[\frac{1}{m_{q'}a} - \frac{5}{4m^3_{q'}a^3}\Big] - \frac{\sqrt{2}G_F m^2_{q'}}{\pi a}\Big[\frac{1+\delta-m^2_h/4m^2_{q'}}{(2+am_h)^2} + \frac{1}{4m^2_{q'}a^2} - \frac{\Omega(S)}{4}\Big\{\frac{1}{m^2_{q'}a^2} - \frac{M^2_Z/m^2_{q'}}{(2+aM_Z)^2}\Big\}\Big]. \quad (27)$$

The first term comes from the kinetic energy, while first and second terms in the second parentheses are from the t-channel Higgs exchange, including the perturbative correction to the Higgs propagator. The rest is from the neutral fictitious scalar exchange in the t-channel. The s-channel neutral fictitious scalar exchange, on the other hand, gives a contribution only for the ($\mathbf{1}$, 1, 0) channel, which is

$$E^{(\mathbf{1},1,0)}_{P^0,s\text{-channel}}[a] = \frac{\sqrt{2}G_F m^2_{q'}}{\pi a}\frac{3}{(1-M^2_Z/4m^2_{q'})}\frac{1}{m^2_{q'}a^2}. \quad (28)$$

As we mentioned, this term always contributes as a positive (repulsive) term in total energy, and it is enhanced by color factor $N_c = 3$. Charged fictitious scalar exchange gives

$$E^{(S)}_{P^+}[a] = \frac{\sqrt{2}G_F m^2_{q'}}{\pi a}\Omega(S)\Big[\frac{1}{2m^2_{q'}a^2} - \frac{M^2_W/2m^2_{q'}}{(2+aM_W)^2}\Big]. \quad (29)$$

Finally, the contribution from one-gluon exchange is

$$E^{(\mathbf{1})}_{\rm QCD}[a] = -\frac{4\alpha_s}{3a}, \qquad E^{(\mathbf{8})}_{\rm QCD}[a] = \frac{\alpha_s}{6a}. \quad (30)$$

With all the terms we have given above, the variational energy in each channel is obtained:

$$E^{(\mathbf{1},0,S)}[a] = E^{(S)}_{\rm com} + E^{(S)}_{P^+} + E^{(\mathbf{1})}_{\rm QCD}, \quad (31)$$

$$E^{(\mathbf{1},1,0)}[a] = E^{(0)}_{\rm com} - E^{(0)}_{P^+} + E^{(\mathbf{1},1,0)}_{P^0,s} + E^{(\mathbf{1})}_{\rm QCD}, \quad (32)$$

$$E^{(\mathbf{1},1,1)}[a] = E^{(1)}_{\rm com} - E^{(1)}_{P^+} + E^{(\mathbf{1})}_{\rm QCD}, \quad (33)$$

for color singlet state, ($\mathbf{1}$, I, S), and

$$E^{(\mathbf{8},0,S)}[a] = E^{(S)}_{\rm com} + E^{(S)}_{P^+} + E^{(\mathbf{8})}_{\rm QCD}, \quad (34)$$

$$E^{(\mathbf{8},1,S)}[a] = E^{(S)}_{\rm com} - E^{(S)}_{P^+} + E^{(\mathbf{8})}_{\rm QCD}, \quad (35)$$

for color octet state, ($\mathbf{8}$, I, S). These results are summarized in the Appendix.

We compute the variational energy $E^{(C,I,S)}[a]$ in each channel and study the properties of the bound states. In the color singlet channels, there always exists a bound state. For small enough $m_{q'}$ the state is very close to the familiar QCD "onium" states. However as $m_{q'}$ increases the parts of the potential proportional to $m^2_{q'}$ become more important. We find the value of a, (in the parameter region given by Eq. (26)) which gives minimum binding energy for fixed $m_{q'}$. (We denote it a_0.) It is compared with the Bohr radius of pure QCD potential, $a_{\rm QCD} \equiv 2\alpha_s/3m_{q'}$. We begin by taking $m_h = 130$ GeV. Later we redo the analysis for the case $m_h = m_{q'}$ which may provide more realistic values of the Higgs mass given the constraints from the stability of the Higgs potential. The results (for $m_h = 130$ GeV) are shown in the upper panel of Fig. 6. From this figure, it can be seen that the size of the singlet bound states are not close to a QCD-like bound state when $m_{q'} \gtrsim 400$ GeV, except for the ($\mathbf{1}$, 1, 0) channel. The sharp break in behavior as $m_{q'}$ increases is due to the limit we impose on the value of a_0 (i.e., it is greater than or equal to $\sqrt{3}/m_{q'}$), which ensures that the relativistic corrections are not too large. In the ($\mathbf{1}$, 1, 0) channel, the contribution from the repulsive s-channel P^0 exchange potential is so large that the bound state has $a_0 > a_{\rm QCD}$ for a range of masses. In the lower panel of Fig. 6, we plot the variational binding energy computed at $a = a_0$ for each color singlet channel.

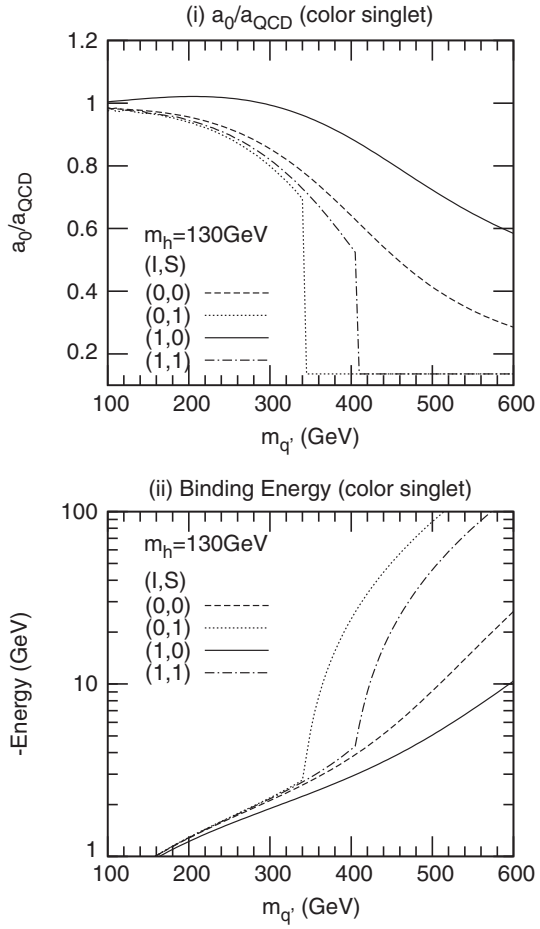

FIG. 6. (i) $a_0/a_{\rm QCD}$ as the function of quark mass in color singlet channels. Here we take $m_h = 130$ GeV and a_0 is the value for which $E[a]$ is minimized (and negative) for fixed quark mass. (ii) Variational binding energy of color singlet channels as the function of the heavy quark mass. Here we set $a = a_0$.

We find binding energies of $O((10–100)\ \text{GeV})$ for $m_{q'} \sim$ 400–500 GeV.

For the color octet channels, on the other hand, bound states do not exist if the heavy fourth generation quark is too light and of course the Higgs Yukawa couplings always play a crucial role because the QCD potential is repulsive. In our numerical analysis, we find the lowest value of $m_{q'}$ for which the minimum of the variational energy $E[a]$ (in the region, $a \geq \sqrt{3}/m_{q'}$) has a negative value. The results are summarized in Table I. Note that the values of the fourth generation quark masses relevant here are not the ones in parenthesis. We find that the lower limit reduces to 440–570 GeV, compared to the one given by the leading order Hamiltonian (i.e., 583 GeV). As in the color singlet channel, we plot the lowest variational binding energy for fixed $m_{q'}$ in Fig. 7. This figure indicates that color octet bound states with a binding energy of $O((10–100)\ \text{GeV})$ exist when $m_{q'} \simeq$ 450–550 GeV. The color octet states we found form color singlet hadrons by neutralizing their color charge at long distances with gluons and light quark-anti quark pairs.

It is important to remember that when a_0 is at the end of the range given by Eq. (26), the actual bound state may be relativistic and more deeply bound than the results presented in this section indicate. Such a situation occurs for the color octet results, except for the $(\mathbf{8}, 0, 0)$ state, and in some of the color singlet channels at larger heavy quark masses. In order to see how our results are affected by the choice of region for a, we consider, for example, the case where the expectation value of $\mathbf{p}^2/m_{q'}^2$ is less than $1/2$, which corresponds to $a \geq \sqrt{2}/m_{q'}$. In Table I, the lower limit on $m_{q'}$ for an octet bound state to exist is also derived using this region for a, instead of Eq. (26) (see the values in parentheses). As it is shown, the limit becomes smaller by 10–20% (except for the $(\mathbf{8}, 0, 0)$ state).

Finally, we give the numerical results in the case of $m_h = m_{q'}$. In the same manner as we did when m_h was fixed at 130 GeV, a_0/a_{QCD} and the binding energy for color singlet channels are given in Fig. 8 and the lower bound on the fourth generation quark mass, and the binding energy for color octet channels are given in Table II and Fig. 9, respectively. For singlet states, the bound state is certainly not QCD-like when $m_{q'} > 400(535)$ GeV in the $(\mathbf{1}, 0, 1)$

TABLE I. Lower limit of quark mass for which a bound state forms in the various color octet channels. We take $m_h =$ 130 GeV. The values in parentheses are given by using $a \geq \sqrt{2}/m_{q'}$ instead of Eq. (26).

(C, I, S)	Lower limit of $m_{q'}$
$(\mathbf{8}, 0, 0)$	574 GeV (574 GeV)
$(\mathbf{8}, 0, 1)$	440 GeV (359 GeV)
$(\mathbf{8}, 1, 0)$	440 GeV (359 GeV)
$(\mathbf{8}, 1, 1)$	510 GeV (439 GeV)

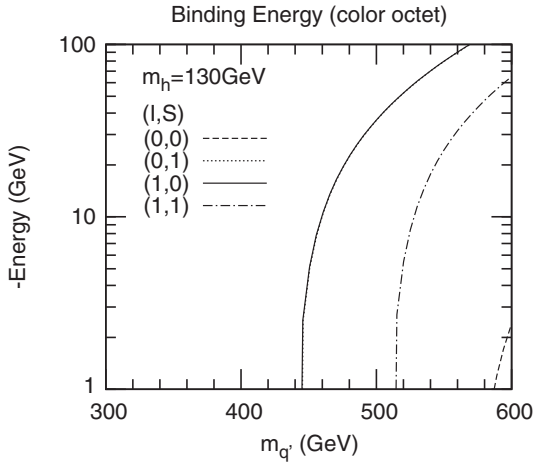

FIG. 7. Variational binding energy of color octet channels plotted as the function of the heavy quark mass. In the plot, we use $m_h = 130$ GeV and take a as the value which gives the lowest binding energy for fixed $m_{q'}$. Note that $(\mathbf{8}, 0, 1)$ and $(\mathbf{8}, 1, 0)$ channels give almost the same results.

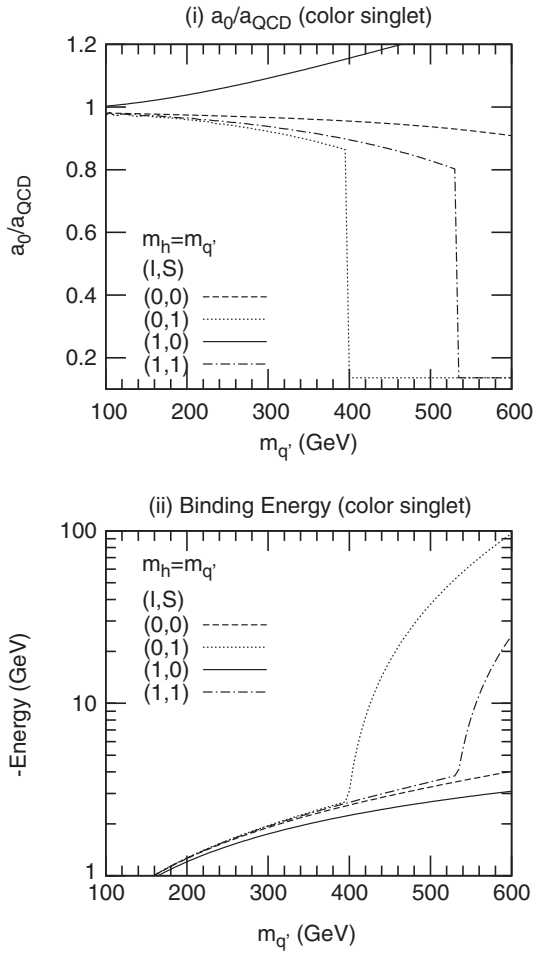

FIG. 8. The same as Fig. 6, except for taking $m_h = m_{q'}$.

TABLE II. The same as Table. I, except for taking $m_h = m_{q'}$.

(C, I, S)	Lower limit of $m_{q'}$
(**8**, 0, 0)	No bound state
(**8**, 0, 1)	534 GeV
(**8**, 1, 0)	534 GeV
(**8**, 1, 1)	696 GeV

((**1**, 1, 1)) channels. On the other hand, octet channels do not form bound state unless $m_{q'} \gtrsim 535$ GeV, which is near the unitarity bound or equivalently strong coupling regime.

We have assumed that $m_{t'} = m_{b'}$ throughout this paper, however it is straightforward to take into account the mass difference between the heavy fourth generation quarks. In that case, the $I = 0$ and 1 sates are no longer the energy eigenstates. Rather we denote the eigenstates by $|+\rangle$ and $|-\rangle$. They are the following linear combinations of the heavy quark isospin eigenstates:

$$|+\rangle \propto |I = 0\rangle + B_+|I = 1\rangle, \tag{36}$$

$$|-\rangle \propto B_-|I = 0\rangle + |I = 1\rangle. \tag{37}$$

Introducing the notation, $m_\pm = m_{t'} \pm m_{b'}$, the energy eigenvalues $E_\pm$ and mixing parameters $B_\pm$ are

$$E_\pm = m_+ + \frac{E^{(C,0,S)} + E^{(C,1,S)}}{2} \pm \sqrt{\left(\frac{E^{(C,0,S)} - E^{(C,1,S)}}{2}\right)^2 + m_-^2}, \tag{38}$$

$$B_+ = \frac{m_-}{m_+ + E^{(C,1,S)} - E_+}, \tag{39}$$

$$B_- = \frac{m_-}{m_+ + E^{(C,0,S)} - E_-}, \tag{40}$$

respectively. When $a_0 \sim a_{\rm QCD}$, m_- is larger in magnitude than $(E^{(C,0,S)} - E^{(C,1,S)})/2$. (Here we are assuming $|m_-| \sim$ 50 GeV.) Then, the mixing parameter is not negligible.

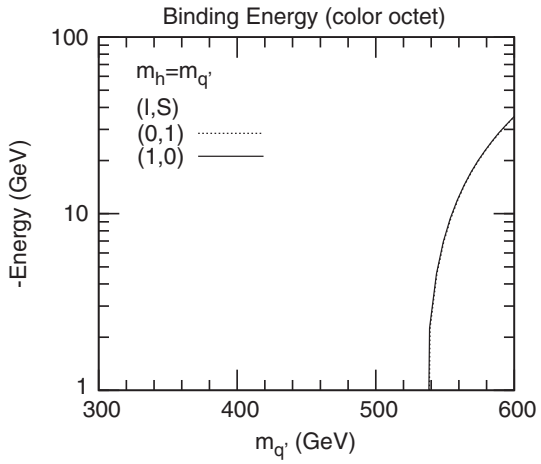

FIG. 9. The same as Fig. 7, except for taking $m_h = m_{q'}$.

On the other hand when a_0 is much smaller than $a_{\rm QCD}$, m_- is not important and the mixing parameter is negligible. Then the states $|\pm\rangle$ are almost isospin eigenstates, i.e., $|+\rangle \simeq |I = 0\rangle$ and $|-\rangle \simeq |I = 1\rangle$. In a more accurate evaluation, one should also take into account the correction m_- makes to $E^{(C,0,S)}$ and $E^{(C,1,S)}$. These corrections are suppressed by (m_-/m_+) and are expected to change the binding energies by a few to 10%.

IV. CONCLUDING REMARKS

Heavy fourth generation quarks may have a long enough lifetime that it is sensible to consider their bound states. At the LHC heavy quark $\bar{q}'q'$ bound states will be produced by gluon fusion. Hence it is important to understand the properties of these states. In this paper we have determined the binding energies and sizes of these states. For $m_{q'} \gtrsim 400$ GeV, the Higgs Yukawa coupling plays a crucial role in the properties of these states and also relativistic and perturbative corrections are important. In a future publication we hope to elucidate more of their properties, including production rates at the LHC and their decay branching ratios.

ACKNOWLEDGMENTS

The work was supported in part by the U.S. Department of Energy under Contract No. DE-FG02-92ER40701, and by the Gordon and Betty Moore Foundation. We are grateful to B. Grinstein for useful discussions.

APPENDIX

Here we give explicit formulas for the variational energy in each channel:

$$E[a]^{(\mathbf{1},0,0)} = \frac{2\sqrt{2}G_F m_{q'}^2}{\pi a^3}\left[-\frac{(1+\delta)a^2}{2(2+am_h)^2} + \frac{1}{4m_{q'}^2} + \frac{m_h^2}{8m_{q'}^2}\frac{a^2}{(2+am_h)^2} - \frac{M_Z^2}{8m_{q'}^2}\frac{a^2}{(2+aM_Z)^2} - \frac{M_W^2}{4m_{q'}^2}\frac{a^2}{(2+aM_W)^2}\right] - \frac{4}{3a}\alpha_s + \frac{1}{a^3}\left[\frac{a}{m_{q'}} - \frac{5}{4m_{q'}^3 a}\right] \tag{A1}$$

$$E[a]^{(\mathbf{1},0,1)} = \frac{2\sqrt{2}G_F m_{q'}^2}{\pi a^3}\left[-\frac{(1+\delta)a^2}{2(2+am_h)^2} - \frac{1}{4m_{q'}^2} + \frac{m_h^2}{8m_{q'}^2}\frac{a^2}{(2+am_h)^2} + \frac{M_Z^2}{24m_{q'}^2}\frac{a^2}{(2+aM_Z)^2} + \frac{M_W^2}{12m_{q'}^2}\frac{a^2}{(2+aM_W)^2}\right] - \frac{4}{3a}\alpha_s + \frac{1}{a^3}\left[\frac{a}{m_{q'}} - \frac{5}{4m_{q'}^3 a}\right] \tag{A2}$$

$$E[a]^{(\mathbf{1},1,0)} = \frac{2\sqrt{2}G_F m_{q'}^2}{\pi a^3}\Bigg[-\frac{(1+\delta)a^2}{2(2+am_h)^2} - \frac{1}{4m_{q'}^2} + \frac{6}{(4m_{q'}^2 - M_Z^2)} + \frac{m_h^2}{8m_{q'}^2}\frac{a^2}{(2+am_h)^2} - \frac{M_Z^2}{8m_{q'}^2}\frac{a^2}{(2+aM_Z)^2} + \frac{M_W^2}{4m_{q'}^2}\frac{a^2}{(2+aM_W)^2}\Bigg] - \frac{4}{3a}\alpha_s + \frac{1}{a^3}\Bigg[\frac{a}{m_{q'}} - \frac{5}{4m_{q'}^3 a}\Bigg] \quad \text{(A3)}$$

$$E[a]^{(\mathbf{1},1,1)} = \frac{2\sqrt{2}G_F m_{q'}^2}{\pi a^3}\Bigg[-\frac{(1+\delta)a^2}{2(2+am_h)^2} - \frac{1}{12m_{q'}^2} + \frac{m_h^2}{8m_{q'}^2}\frac{a^2}{(2+am_h)^2} + \frac{M_Z^2}{24m_{q'}^2}\frac{a^2}{(2+aM_Z)^2} - \frac{M_W^2}{12m_{q'}^2}\frac{a^2}{(2+aM_W)^2}\Bigg] - \frac{4}{3a}\alpha_s + \frac{1}{a^3}\Bigg[\frac{a}{m_{q'}} - \frac{5}{4m_{q'}^3 a}\Bigg] \quad \text{(A4)}$$

$$E[a]^{(\mathbf{8},0,0)} = \frac{2\sqrt{2}G_F m_{q'}^2}{\pi a^3}\Bigg[-\frac{(1+\delta)a^2}{2(2+am_h)^2} + \frac{1}{4m_{q'}^2} + \frac{m_h^2}{8m_{q'}^2}\frac{a^2}{(2+am_h)^2} - \frac{M_Z^2}{8m_{q'}^2}\frac{a^2}{(2+aM_Z)^2} - \frac{M_W^2}{4m_{q'}^2}\frac{a^2}{(2+aM_W)^2}\Bigg] + \frac{1}{6a}\alpha_s + \frac{1}{a^3}\Bigg[\frac{a}{m_{q'}} - \frac{5}{4m_{q'}^3 a}\Bigg] \quad \text{(A5)}$$

$$E[a]^{(\mathbf{8},0,1)} = \frac{2\sqrt{2}G_F m_{q'}^2}{\pi a^3}\Bigg[-\frac{(1+\delta)a^2}{2(2+am_h)^2} - \frac{1}{4m_{q'}^2} + \frac{m_h^2}{8m_{q'}^2}\frac{a^2}{(2+am_h)^2} + \frac{M_Z^2}{24m_{q'}^2}\frac{a^2}{(2+aM_Z)^2} + \frac{M_W^2}{12m_{q'}^2}\frac{a^2}{(2+aM_W)^2}\Bigg] + \frac{1}{6a}\alpha_s + \frac{1}{a^3}\Bigg[\frac{a}{m_{q'}} - \frac{5}{4m_{q'}^3 a}\Bigg] \quad \text{(A6)}$$

$$E[a]^{(\mathbf{8},1,0)} = \frac{2\sqrt{2}G_F m_{q'}^2}{\pi a^3}\Bigg[-\frac{(1+\delta)a^2}{2(2+am_h)^2} - \frac{1}{4m_{q'}^2} + \frac{m_h^2}{8m_{q'}^2}\frac{a^2}{(2+am_h)^2} - \frac{M_Z^2}{8m_{q'}^2}\frac{a^2}{(2+aM_Z)^2} + \frac{M_W^2}{4m_{q'}^2}\frac{a^2}{(2+aM_W)^2}\Bigg] + \frac{1}{6a}\alpha_s + \frac{1}{a^3}\Bigg[\frac{a}{m_{q'}} - \frac{5}{4m_{q'}^3 a}\Bigg] \quad \text{(A7)}$$

$$E[a]^{(\mathbf{8},1,1)} = \frac{2\sqrt{2}G_F m_{q'}^2}{\pi a^3}\Bigg[-\frac{(1+\delta)a^2}{2(2+am_h)^2} - \frac{1}{12m_{q'}^2} + \frac{m_h^2}{8m_{q'}^2}\frac{a^2}{(2+am_h)^2} + \frac{M_Z^2}{24m_{q'}^2}\frac{a^2}{(2+aM_Z)^2} - \frac{M_W^2}{12m_{q'}^2}\frac{a^2}{(2+aM_W)^2}\Bigg] + \frac{1}{6a}\alpha_s + \frac{1}{a^3}\Bigg[\frac{a}{m_{q'}} - \frac{5}{4m_{q'}^3 a}\Bigg]. \quad \text{(A8)}$$

[1] T. Aaltonen *et al.* (CDF Collaboration), Phys. Rev. Lett. **104**, 091801 (2010); C. J. Flacco, D. Whiteson, and M. Kelly, arXiv:1101.4976.
[2] G. D. Kribs, T. Plehn, M. Spannowsky, and T. M. P. Tait, Phys. Rev. D **76**, 075016 (2007).
[3] H. J. He, N. Polonsky, and S. F. Su, Phys. Rev. D **64**, 053004 (2001).
[4] B. Holdom, Phys. Rev. D **54**, R721 (1996).
[5] J. Erler and P. Langacker, Phys. Rev. Lett. **105**, 031801 (2010).
[6] M. S. Chanowitz, Phys. Rev. D **82**, 035018 (2010).
[7] O. Eberhardt, A. Lenz, and J. Rohrwild, Phys. Rev. D **82**, 095006 (2010).
[8] M. S. Chanowitz, M. A. Furman, and I. Hinchliffe, Phys. Lett. B **78**, 285 (1978).
[9] M. S. Chanowitz, M. A. Furman, and I. Hinchliffe, Nucl. Phys. **B153**, 402 (1979).
[10] M. S. Chanowitz, Phys. Lett. B **352**, 376 (1995).
[11] R. F. Dashen and H. Neuberger, Phys. Rev. Lett. **50**, 1897 (1983).
[12] M. B. Einhorn and G. J. Goldberg, Phys. Rev. Lett. **57**, 2115 (1986).
[13] P. H. Frampton, P. Q. Hung, and M. Sher, Phys. Rep. **330**, 263 (2000).
[14] M. Hashimoto, Phys. Rev. D **81**, 075023 (2010).
[15] P. Fileviez Perez and M. B. Wise, Phys. Rev. D **82**, 011901 (2010).
[16] P. Q. Hung and C. Xiong, Nucl. Phys. **B847**, 160 (2011).
[17] P. Q. Hung and C. Xiong, Phys. Lett. B **694**, 430 (2011); arXiv:1012.4479.
[18] B. Holdom, W. S. Hou, T. Hurth, M. L. Mangano, S. Sultansoy, and G. Unel, PMC Phys. A **3**, 4 (2009).
[19] B. Holdom, Phys. Lett. B **686**, 146 (2010).
[20] A. V. Manohar and I. W. Stewart, Nucl. Phys. B, Proc. Suppl. **94**, 130 (2001); *HEAVY FLAVOR PHYSICS: Ninth International Symposium on Heavy Flavor Physics*, AIP Conf. Proc. No. 618, (AIP, New York, 2002).
[21] A. V. Manohar and I. W. Stewart, Phys. Rev. D **62**, 074015 (2000).